

CHARACTERISTICS OF SURFACE MOTION ON A TOPOGRAPHIC IRREGULAR GROUND DURING LARGE EARTHQUAKES

Kaeko YAHATA¹, Toru SASAKI², Masanori NIWA³ And Tsunehisa TSUGAWA⁴

SUMMARY

Different acceleration records of the surface motion were observed at two adjacent observation stations during the Kushiro-Oki Earthquake on January 15, 1993, one of which was set up on the building foundation of the Kushiro Meteorological Observatory (JMA) and the other was on the ground (site1). As the area of the station is located on a hill, in order to investigate the reason why the amplitude discrepancy between the two nearby observation stations occurred, two vertical array stations were set up after the earthquake. Analytical studies by applying one and two dimensional models considering a nonlinear soil behavior were carried out for the strong motions recorded at both stations during the Hokkaido-Toho-Oki Earthquake on October 4, 1994.

Two-dimensional model can be applicable to demonstrate the different surface motions at two sites which are generated by the influence of the topographic cliff during a large earthquake.

It is also clarified by using the same model for the case of the Kushiro-Oki Earthquake that the large amplification of the surface motion at JMA is produced by the influence due to the first resonance frequency of the soil-structure interaction close to 2.5Hz. Moreover, the presence of the topographic cliff gives much affection to the surface amplification in the higher frequencies above 5Hz.

INTRODUCTION

Different characteristic amplifications of the surface motion during Kushiro-Oki Earthquake (EQ.1, hereafter) were observed at two acceleration observation stations within the area of the Kushiro Meteorological Observatory in Hokkaido on January 15, 1993. The area is located on a hill as shown in Fig.1 which indicates the plan view and two orthogonal cross sections. The location of two stations is shown in Fig.2, one of which was set up on the building foundation at JMA and the other was on the ground (site1). The observed acceleration amplitudes during EQ.1 were roughly 900 Gal and 700 for JMA and site1, respectively. In order to investigate the influence of the topographic cliff on the surface motion amplification, two vertical array stations sites 1 and 2 as shown in Fig.2 were set up after EQ.1

As the strong motions were recorded at both stations during the Hokkaido-Toho-Oki Earthquake on October 4, 1994 (EQ.2 hereafter), firstly the studies based on the observations during EQ.2 will be carried out and then the surface motions during EQ.1. The main purpose of this paper is to clarify the reason why the discrepancy between the amplifications of the surface motion at two stations during EQ.1 was yielded. The discrepancy may associate with the influence due to the topographic cliff and the soil nonlinearity.

OUTLINE OF THE EARTHQUAKE OBSERVATION SYSTEM

The plane view of the seismographs on the surface is shown in Fig.3 and the soil profiles of the both sites are

¹ Kajima Technical Research Institute, Tokyo, Japan Email:kaeko@katri.kajima.co.jp

² Kajima Technical Research Institute, Tokyo, Japan Email:sasakit@katri.kajima.co.jp

³ Kajima Technical Research Institute, Tokyo, Japan Email:niwa@katri.kajima.co.jp

⁴ Kajima Technical Research Institute, Tokyo, Japan Email:tsugawa@katri.kajima.co.jp

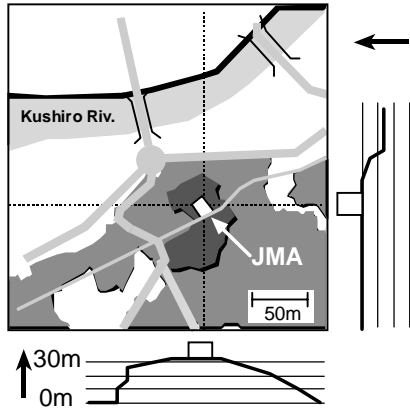


Figure1: Topography around

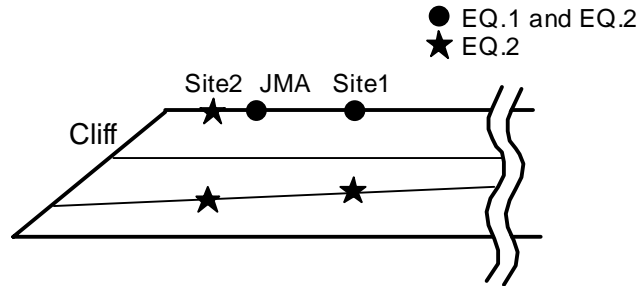


Figure2: Location of the observation stations

shown in Fig.4. While the directions of the seismographs in both sites are at N063 and N153, respectively and they are placed on the ground, for the case of JMA, it is at N0 and N90, respectively and it is placed on the building foundation of the Kushiro Meteorological Observatory.

Since November 1993, earthquakes have been monitored by the strong - motion accelerometers on the array observation system. The ground motions during EQ.2 as shown in Table1 were observed at sites 1 and 2.

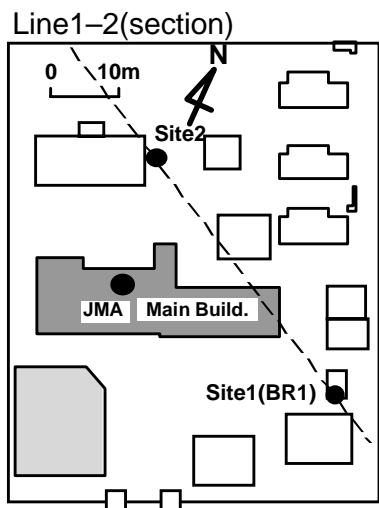


Figure3: General view of Kushiro JMA

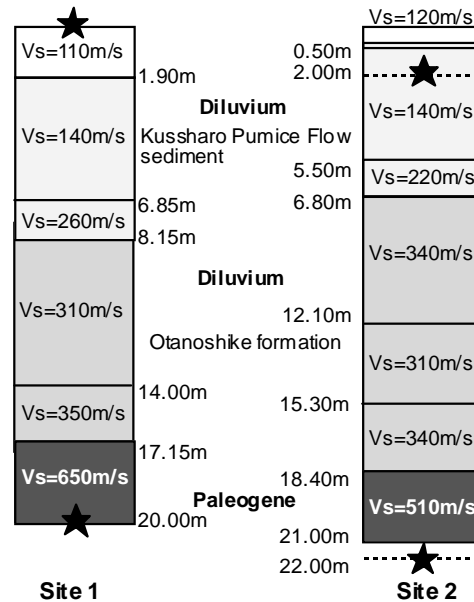


Figure4: Soil condition of 2 boreholes

Table1 Hokkaido-Toho-Oki Earthquake (EQ.2) (1994)

Date	Epicenter	Distance (km)	Depth (km)	MJ	IJ	A.max (cm/s/s)					
						Site1:above		Site2:below		UD	
						063 (G.L.)	063 (G.L.-20)	153 (G.L.)	153 (G.L.-20)	UD (G.L.)	UD (G.L.-20)
10/4	East off Hokkaido	270	30	8.1	6	314.1	100.2	392.2	94.8	189.2	74.4
						402.6	119.0	258.3	95.4	178.6	77.6

Note; Site2:G.L.-2m, G.L.-22m

DISCUSSIONS ON EQ.2

Observation

The Spectrum ratios of the observed waves at the surfaces to those of the boreholes at sites 1 and 2 are shown in Fig.5. The response tendencies at both sites are similar for frequencies below 5Hz and the first resonance peaks for sites 1 and 2 appear at frequencies 3.8Hz and 3.7Hz, respectively. However, the discrepancy between the responses at both sites is noticeable with increasing frequencies, especially for frequency range from 6Hz to 8Hz and the amplitude of the second resonance peak of site2 which is estimated to be at frequency near 7Hz is invisible.

A previous investigation¹⁾ on 14 other earthquakes observed in the same array system pointed out a high frequency discrepancy between both sites.

Analysis

As for numerical analysis, first the results obtained from the one-dimensional nonlinear analysis will be discussed to clarify the availability of the analysis for simulating the observations of both sites. Then two-dimensional FEM analysis will be introduced to reproduce it.

DYNAFLOW²⁾ is used as the analytical code in which soil nonlinearity is estimated as H-D model and the mesh size of the model is effective in the frequencies below 10Hz. The variable as shown in Fig.4 is adopted as the initial stiffnesses at sites 1 and 2, respectively.

One-dimensional analysis

The observed waves at the boreholes are applied into the bases of the models equal to the observation levels at sites 1 and 2 respectively as the input motions. Fig.6 shows the analytical results corresponding to the observations as shown in Fig.5. Fig.7 shows the analytical and observed accelerations of both sites with a large amplitude range. The spectral tendencies of sites 1 and 2 in Fig.6 are similar. From comparisons between Figs 5 and 6 for the case of site2, the high frequency range is not fit by the analysis. The reason why the one-dimensional model is not effective for the case of site2 may be that the surface ground motion there is more sensitive to the presence of the cliff than the case of site1 because of the closer distance. As for the Fig.7, the analysis reproduces approximately the observed wave at site 1, but significantly less so at site 2.

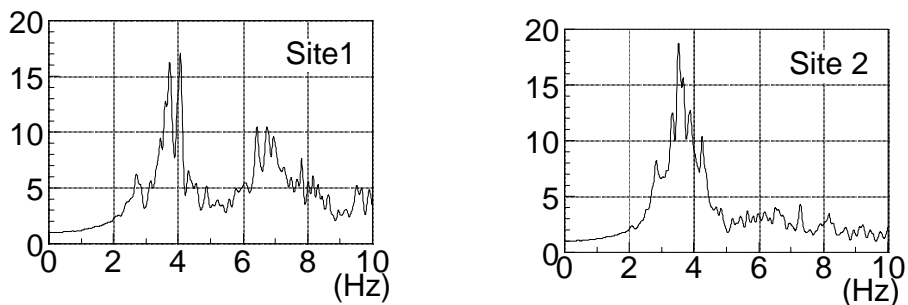


Figure5: Spectrum Ratio of Hokkaido-Toho-Oki Earthquake in the observation (EQ.2)

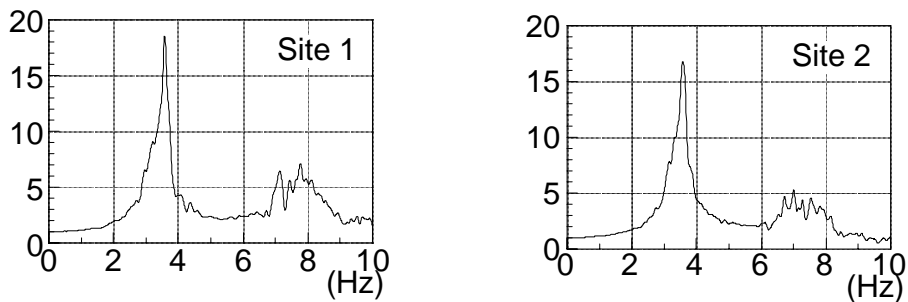


Figure6: Spectrum Ratio of Hokkaido-Toho-Oki Earthquake in the analysis (EQ.2)

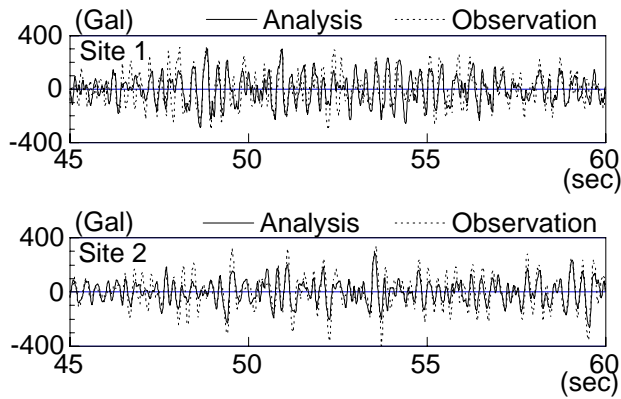


Figure7: Comparison of time histories during Hokkaido-Toho-Oki Earthquake between observation and analysis (EQ.2)

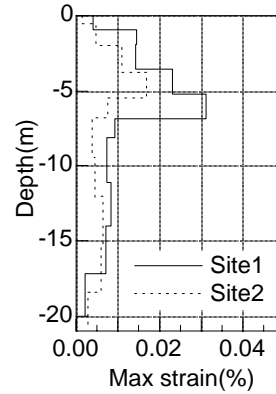


Figure8: Maximum shear strain distributions

In order to estimate soil nonlinearity during EQ.2, the maximum shear strain distributions in the analysis at both sites were obtained and are drawn in Fig.8. The tendencies of the strain distributions at both sites are similar. The large strain amplitudes, being roughly $1.5E10^{-3}$, at both sites occurs in the layers near the surface where their stiffnesses are small, therefore the surface ground motions during EQ.2 may be depend upon soil nonlinearity. But the comparison of the general tendency between the strain distribution at both sites indicates that the contribution of the different soil profiles between both sites has negligible effect on the observed surface motions.

Two-dimensional analysis

The two-dimensional model in Fig.9 shows how the geological profile of the cliff is included to investigate the surface amplification. This profile approximates a cross section of the ground along line 1 - 2 in Fig.3, and the boundary conditions of the side and the base are roller and viscous damping respectively. The directions of the waves in two-dimensional analysis are transformed from the observed waves into those for the plane along Line1-2. Although the observed wave at site 1 is recorded at G.L.-20m, the wave at the borehole of site 1 is input into the model base at G.L.-30m. The reasons why the observed wave is used for input motion are as follows.

- * Through the study of one-dimensional analysis, the ground motion at site1 during EQ.2 can be assumed as the motion obtained from one dimension theory.
- * As the stiffness of the third layer as shown in Fig.9 is large, the difference between the observed waves at G.L.-20m and G.L.-30m is probably small.
- * Compared with the waves obtained from iterative analysis using one-dimensional nonlinear soil model, the observed wave can be substituted directly.

The spectrum ratios obtained from two-dimensional analysis are shown in Fig.10 and should be compared to those of Figs.5 and 6.

The agreement between the spectrum ratios of the observation and the analysis is better than those in Fig.6 as described below for reproducing the amplification effect from the scattering due to the topographic cliff.

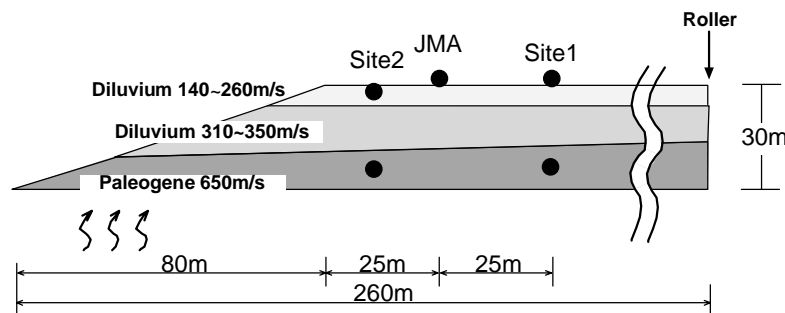


Figure9: Analytical model of two-dimension

- * The first peaks of both sites in Fig.10 can simulate such tendencies as the observation peaks near 3.5Hz are not single, but complex configurations.
- * The discrepancy between the amplitudes of sites 1 and 2 at second peaks in the observations is fit by the two dimensional model for a wide range of frequencies.

Since the two-dimensional model fits the observed surface amplifications for EQ.2 reasonably well, the observations at the JMA site during EQ.1 will be analyzed by using the same model.

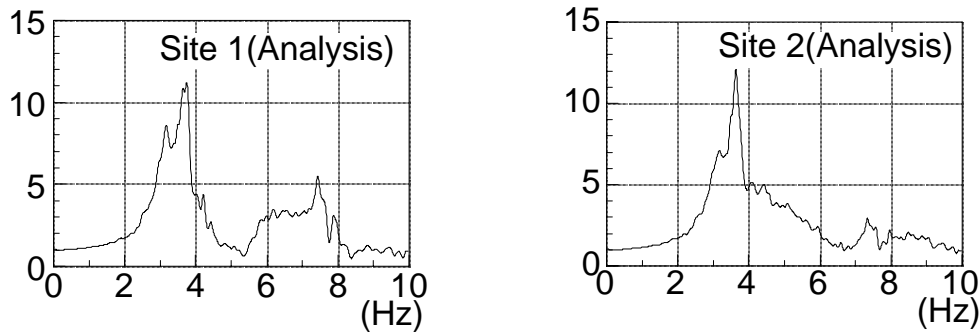


Figure10: Spectrum ratio of Hokkaido-Toho-Oki Earthquake in two-dimensional analysis (EQ.2)

KUSHIRO-OKI-EARTHQUAKE (EQ.1)

In order to estimate the surface amplification at site1 and JMA during EQ.1, the input motion used in the analytical model at site1 should be calculated by an iteration method ³⁾ because there were only two observation points on the surface. (Refer to Fig.2)

After calculating the input motion, firstly the analysis using the soil model as shown in Fig.9 is carried out and then a two dimensional analysis by using similar model to Fig.9 is also done for simulating the observations. The latter model includes a soil-structure interaction of the building at JMA, but in which some distance from Line 1 - 2 as shown in Fig.3 is neglected.

Input motion

The procedure to obtain the input motion is briefly described below.

Incident wave at G.L.-30m of site 1 is calculated with linear analysis using the observed wave at the surface based on a one-dimensional soil model. A trial and error interaction procedure is continued until the calculated wave agrees approximately with the observed wave on the surface. The calculation employs a one-dimensional nonlinear soil model in which the incident wave above is first applied at G.L.-30m and then repeatedly modified.

The incident wave at G.L.-30m obtained from nonlinear analysis is shown in Fig.11-1 while the observed and the calculated waves at the surface are also shown in Figs.11-2 and 11-3, respectively. The agreement between the latter waves is excellent, so the incident wave estimated in the method may be applicable to the two-dimensional analysis. At site 1, the maximum shear strain for EQ.1 in Fig.12 is greater than it for EQ.2 in Fig. 8, but, qualitatively, the two figures are similar.

Soil model

After carrying out the two-dimensional analysis, the obtained spectral amplifications at sites 1 and 2 are shown in Fig.13 and the maximum shear distributions at both sites are also shown in Fig.14. Findings are as follows.

Soil nonlinearity gives much affection to the surface amplifications at sites 1 and 2 because the first peaks move to the lower frequencies and their amplitudes become less than those during EQ.2. The similar discrepancy between the amplitudes of both sites in the frequencies of 6Hz ~ 8Hz to that for the case of EQ.2 still remains. The strain amplitudes increase from the results of one-dimensional analysis as shown in Fig.12, however, their distributions are similar for one- and two-dimensions.

Soil-structure interaction model

Since the seismograph at JMA was on the building's foundation, the soil-structure interaction model ⁴⁾ in Fig.15 is added to the soil model at JMA to examine the characteristic amplification during EQ.1. Particular attention is given to the interpretation of the difference in observed surface amplifications between JMA and site 1. The spectrum ratios of the observation and analysis at JMA for site 1 are shown in Figs.16 and 17, respectively. They are estimated using the waves within the interval of the large acceleration amplitudes at the surface waves. Fig.18 shows the same ratio obtained from the soil model. The findings in these three figures are as follows.

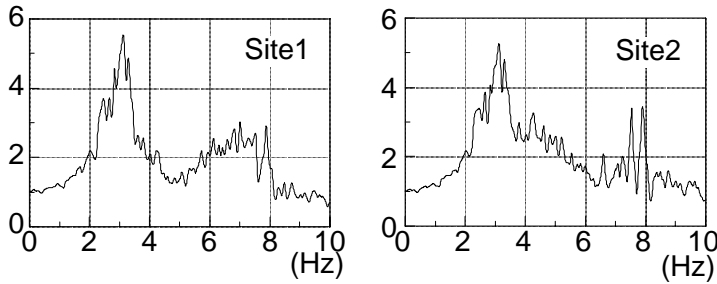


Figure13: Spectrum ratio of Kushiro-Oki Earthquake in two-dimensional analysis (EQ.1)

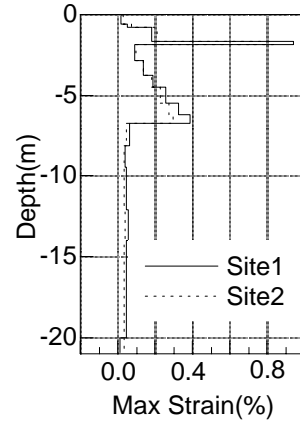


Figure14: Maximum shear strain distribution

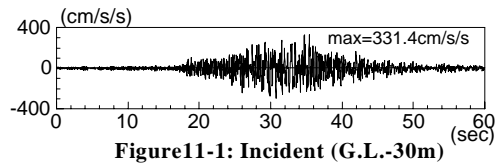


Figure11-1: Incident (G.L.-30m)

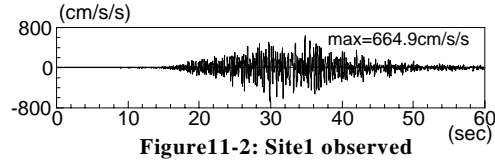


Figure11-2: Site1 observed

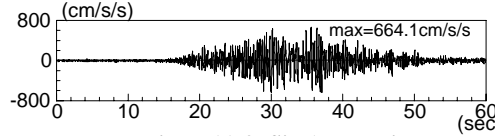


Figure11-3: Site1 analysis

Figure11: Time history waves of Kushiro-Oki Earthquake

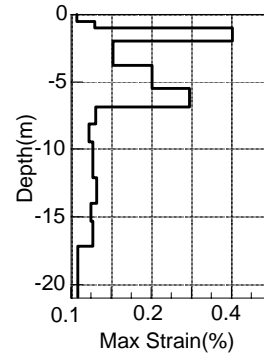


Figure12: Maximum shear strain distribution

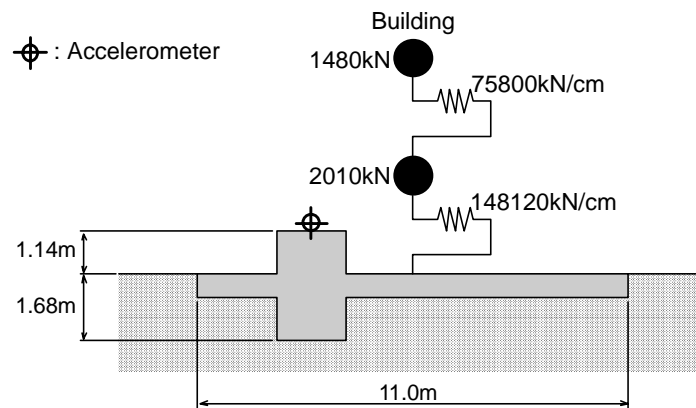


Figure15: Model of soil-foundation-structure interaction

The analytical results of the interaction model can demonstrate the observed tendency at JMA, however, a discrepancy in amplitude between both results is seen. There are three peaks in Figs.16 and 17, but only two peaks for the soil model in Fig.18. The latter probably correspond to the second and the third peaks in Fig.16. These two peaks may be generated by the different surface amplifications from the soil model at JMA and site 1 above 5Hz as shown in Fig.13 due to an influence of the topographic cliff. A comparison of three and two peaks

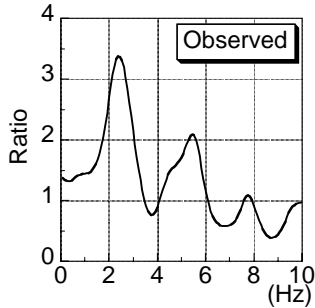


Figure16: Spectrum ratio

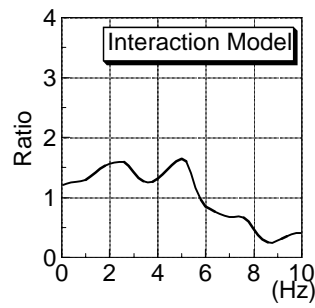


Figure17: Spectrum ratio of soil

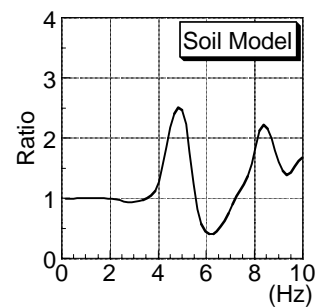


Figure18: Spectrum ratio

-structure interaction

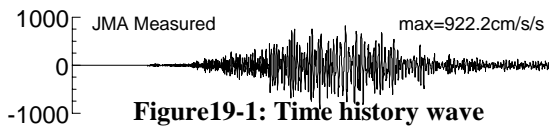


Figure19-1: Time history wave

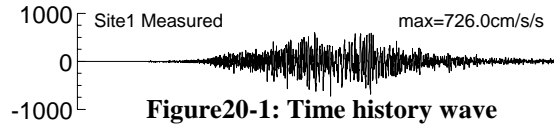


Figure20-1: Time history wave

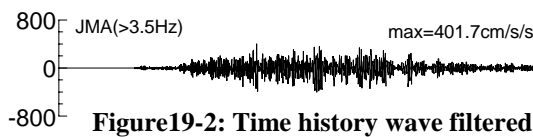


Figure19-2: Time history wave filtered

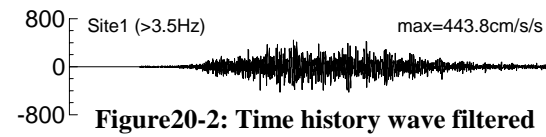


Figure20-2: Time history wave filtered

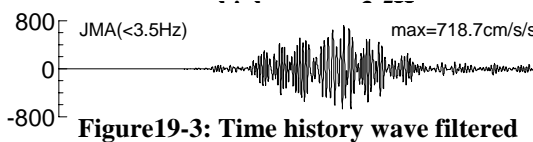


Figure19-3: Time history wave filtered

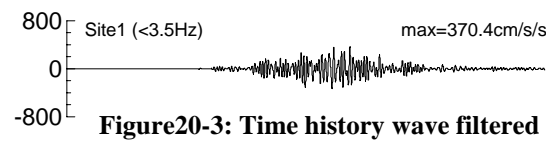


Figure20-3: Time history wave filtered

Figure19: Observation at JMA

Figure20: Observation at Site1

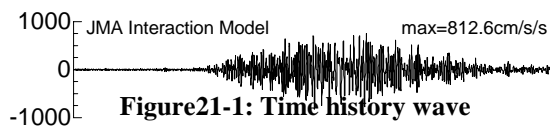


Figure21-1: Time history wave

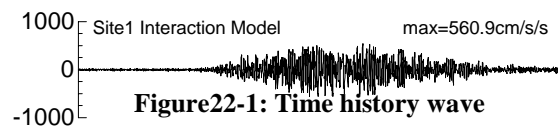


Figure22-1: Time history wave



Figure21-2: Time history wave filtered

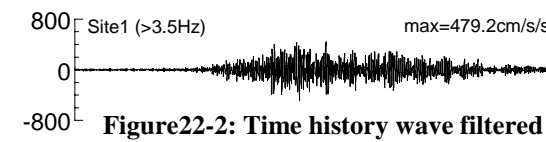


Figure22-2: Time history wave filtered

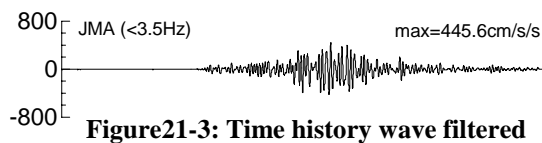


Figure21-3: Time history wave filtered

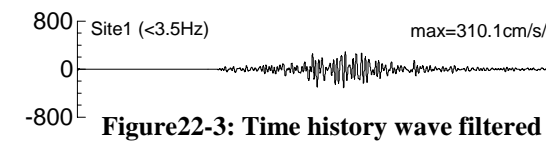


Figure22-3: Time history wave filtered

Figure21: Analysis at JMA (sec)

Figure22: Analysis at Site1 (sec)

in each model suggests that the first resonance frequency in Figs.16 and 17 may result from the effect of the soil-structure interaction system at JMA.

To understand how the occurrence of the first peak due to the interaction influence plays a role in the amplification at JMA, low/high pass filters are applied into the time history waves at JMA and site 1 for the observation and the analysis. Fig.19 shows three types of the observed waves at JMA: the original, after the 3.5Hz high-pass filter, and after the 3.5Hz low-pass filter. A similar set of three waves for site 1 are also shown in Fig.20. As for the analysis of the interaction models, three kinds of waves for JMA and site 1 are shown in Figs.21 and 22. The filter at 3.5Hz is suitable to point out the influence of the first resonance peak close to 2.5Hz on the surface amplification because the amplitudes in the frequencies near 3.5Hz are less affected by the amplification from the peaks as shown in Fig.13.

The amplitude of the original observation at JMA is greater than that for site 1 as shown in Figs.19-1 and 20-1, and for the case of the low pass filter, the former is greater than the latter. On the other hand, for the case of the high pass filter, the difference in amplitude between JMA and site 1 is slight. Through these observations, it is concluded that the amplification property of frequencies below 3.5Hz produces a greater surface motion at JMA than that at site 1, and such phenomenon may be caused by an influence from the first resonance peak in the nonlinear soil-structure interaction.

Three kinds of time history in the analysis corresponding to Figs.19 and 20 are shown in Figs.21 and 22, respectively. The waves of Figs.21-1 and 22-1 without any filters can reproduce the observations of Figs.19-1 and 20-1. The relative relations for the high- and low-pass waves of JMA and site 1 in the analysis agrees with those of the observation. It may be explained from the analytical results that the first resonance frequency near 2.5Hz significantly affects the surface motion amplification at JMA.

CONCLUSIONS

Through the comparisons between observation and analysis at sites 1, 2, and JMA for EQ.1 and EQ.2, several conclusions are as follows;

1. The surface amplifications are greatly influenced by the topographic cliff in the higher frequencies above 5Hz.
2. Soil nonlinearities occurred during EQ.1 and EQ.2, and the maximum shear amplitudes of the soil during EQ.1 are greater than that of EQ.2.
3. The two dimensional analytical model can interpret the differences in the observed surface amplifications caused by the effect of the topographic cliff as well as the nonlinear effect of the soil during a large earthquake.
4. It is clarified that the observed discrepancy between the surface amplifications at site 1 and JMA during EQ.1 is caused by the influence of the first resonance frequency below 3.5Hz in the soil-structure interaction.

REFERENCES

- 1) Ishida, H., Sasaki, T., Niwa, M., Y. Kitagawa, Y. and Kashima, T. (1996), "Amplification characteristics of surface layers obtained from earthquake observation records of vertical instrument arrays at Kushiro local meteorological observatory", *J. Struct. Constr. Engng., AIJ, No. 490*, pp91-100. (in Japanese)
 - 2) Prevost, J. H. (1978), "Plasticity Theory for Soil Stress-Strain Behavior", *J. Eng. Mech. Div., ASCE, Vol.104*
 - 3) Tobita, J. et al. (1994), "Estimation of Ground Motion in Kushiro City During 1993 Kushiro-Oki-Earthquake", *9th JEES*, pp409-414 (in Japanese)
- Dan, K., Watanabe, K., Kikuchi, M., Ebihara, M. (1993), "Structural damage potential of strong-motion records at the Kushiro district meteorological observatory from the 1993 Kushiro-Oki-Earthquake(M7.8)", *J. Struct. Constr. Engng., AIJ, No.454*, pp51-60. (in Japanese)